Available online at www.sciencedirect.com
ScienceDirect
Thermochimica Acta 471 (2008) 1–6
thermochimica acta
www.elsevier.com/locate/tca

Review

Liquidus temperatures determination of the dispersed binary system

A. Jamil, T. Kousksou *, Y. Zeraouli, J.-P. Dumas

Laboratoire de Thermique Energétique et Procédés Avenue de l'Université, BP1155-64013 Pau Cedex, France

Received 20 November 2007; received in revised form 31 January 2008; accepted 7 February 2008
Available online 15 February 2008

Abstract

In this research, based on the work of Jamil et al. [A. Jamil, T. Kousksou, Y. Zeraouli, J.P. Dumas, E. Schall, Isothermal and non-isothermal melting of the binary solution inside an emulsion. Thermochim. Acta 460 (2007) 22–27], an experimental method and numerical simulations were developed to determine the liquidus temperatures of the dispersed binary solution. The method is based on the analysis of the DSC curves. The liquidus temperatures as functions of component composition are found to be in good agreement with some available literature data.

Keywords: Solid–liquid equilibrium; DSC; Heat transfer; Binary solution; Emulsion

Contents

1. Introduction

Mixtures of aqueous salts are considered as useful latent energy storage materials. They are storing heat as the solid–liquid phase transition enthalpy, and are widely applied to maintain constant temperature environment for the reservation of food and pharmaceuticals [2–4]. Solid–liquid phase equilibria (SLE) data are essential in designing apparatus and operation of industrial using these mixtures because they determine the possibility to predict the percentage of the latent energy stored inside the process [5].

Differential scanning calorimetry (DSC) is one of the most effective methods for mapping a liquid–solid phase diagram for a binary system. Since the DSC curve depends on the shape of liquidus and solidus curves. The total DSC curve must be evaluated to obtain more accurate SLE.

Various methods have been proposed to determine the solid–liquid-phase equilibria [6,7]. Most of these researches based on the onset and the peak temperatures obtained from the measured DSC curves. Huang and Chen [8] proposed a deconvolution method to predict the solid–liquid equilibria of the organic binary mixtures. Their method used the experiment and the theoretical calculations to detect the fractional transformation of solid–liquid equilibrium of organic mixture. Recently, Takiyama et al. [5] developed a new technique to determine the SLE for organic systems. They simulate DSC curves by using the solid–liquid equilibrium and compares the simulated DSC curves with the measured DSC curves, and then, the phase diagram is modified automatically to provide agreement between them.

In the solid–liquid-phase equilibria, the transformed fraction $(0 \leq X \leq 1)$ is always regarded as an important property

* Corresponding author.
E-mail address: Tarik.kousksou@univ-pau.fr (T. Kousksou).

0040-6031/$ – see front matter © 2008 Elsevier B.V. All rights reserved.
doi:10.1016/j.tca.2008.02.003

Nomenclature

P	mass fraction of the dispersed substance
T	temperature (°C)
T_{peak}	peak maximum temperature (°C)
X	transformed fraction
X_E	eutectic concentration

Greek letters

β	heating rate (K min^{-1})
Φ	specific heat flow rate (W g^{-1})

Subscripts

a	antifreeze
end	end temperature
f	emulsifying medium
i	initial
plt	plate
s	solution

of the samples. It always was used to evaluate the kinetics of the transformation and the phase transformation rate. It is difficult to directly obtain transformed fraction from the experimental measurement.

Sassi et al. [9] and Siffrini [10] have realized a simplified model to simulate a melting of saline binary solution by assuming the uniformity of the sample temperature. The results of this model are qualitative and do not permit to find the shape of the experimental thermograms.

In the previous work [1], we have presented a physical model concerning the heat transfer in the case of a phase change of binary solution dispersed within emulsions. The objective was to describe the thermal transfer inside these dispersions and to determine the space–time distribution of temperature and the local proportion of the transformed droplets in the sample. The model is based on the resolution of the energy equation with a heat source depending on the local difference between the solution temperature T_s and the temperature of the emulsifying medium T_f. The effect of the heating rate β, the initial mass fraction of the solute $X_{a,i}$, the mass fraction of the dispersed saline binary solution P and the sample mass m on the kinetics of the melting process was examined. The present research shows how the liquidus temperatures of the dispersed binary solution can be constructed by using differential scanning calorimetry.

2. Experimental

The investigated sample is NH_4Cl–H_2O binary eutectic system. It is dispersed by a high-speed stirrer within an emulsifying medium made of a mixture of paraffin oil and lanolin.

Thermal analysis was carried out using a PYRIS DIAMOND DSC of PerkinElmer. The temperature scale of the instrument was calibrated by the melting point of pure ice (273.15 K or 0 °C) and mercury (234.32 K or −38.82 °C). The principle of the power-compensation used in dispersed droplet is widely detailed in Refs. [11,12].

We have already presented the experimental cell in Ref. [1], which consists of a cylindrical cell of height $Z_0 = 1.1$ mm and radius $R = 2.215$ mm.

3. Results and discussions

A physical model to predict the isothermal and non-isothermal melting of the binary solution inside an emulsion has been developed and reported by the writers [1] and it is deemed to repeat it in the present work. This model described with accuracy the shape of the thermograms.

The purpose of this paper is to show the applicability of the proposed model to determine the relation between the thermogram and the liquidus temperature of the dispersed solution.

Fig. 1 shows a typical DSC curve of the eutectic mixture. The DSC curve exhibits isothermal eutectic and non-isothermal solid–liquid transition peaks. The same figure presents also, a typical plot of the transformed fraction curve of NH_4Cl–H_2O system. The transformed fraction represents the reaction fraction of solid–liquid equilibrium transition.

Using the proposed model we can easily determined the end point of both the eutectic transformation T_{end1} and the progressive melting T_{end2} (see Fig. 1). We can also predict the variation of the temperatures T_f and T_s in the center of the cell versus T_{plt} (see Fig. 2).

3.1. Effect of the heating rate β

Fig. 3 displays the prediction of temperatures T_f and T_s in the center of the sample and the transformed fraction (Fig. 4) for different heating rates. Despite the small dimensions of the sample, we have found important temperature gradients, responsible for the shape of the peaks. These gradients become more and more important as heating rate increases.

Fig. 5 shows the influence of the heating rate on T_{end1} and T_{end2}. We can note that both temperatures increase continuously

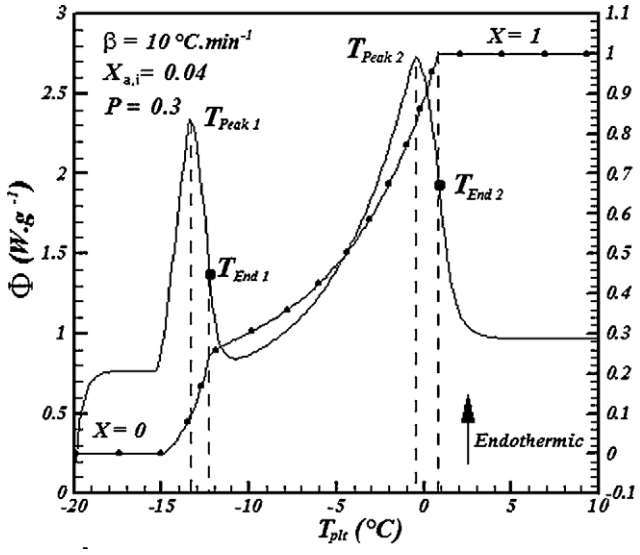

Fig. 1. Typical thermogram for the melting of the eutectic mixture.

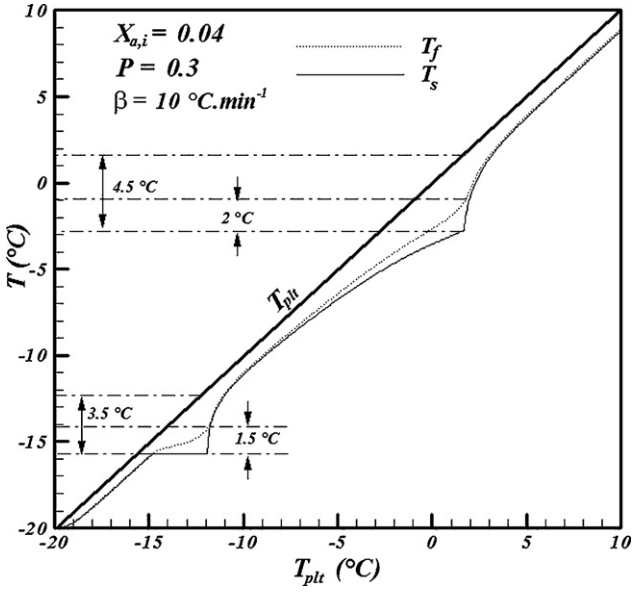

Fig. 2. T_f and T_s in the centre of the sample for $P = 0.3$, $X_{a,i} = 0.4$ and $\beta = 10\,^{\circ}\mathrm{C\,min^{-1}}$.

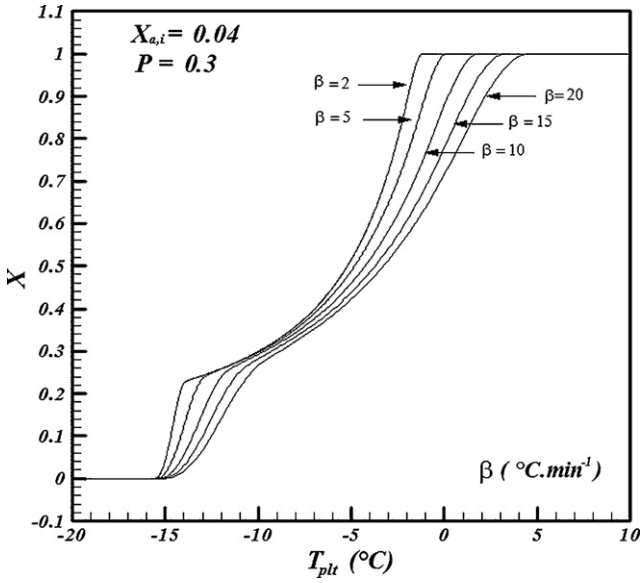

Fig. 4. Effect of the heating rate β on X in the center of the sample.

with increasing heating rate. This increase is likely attributed to the overall thermal resistance between the sample and the DSC plate.

From Fig. 5 it is found that for different heating rates, the instant of the end point of the progressive melting inside the sample coincides with the real equilibrium temperature of the initial mixture $T_{eq}(X_{a,i})$. This result is natural because the end point of the transformation corresponds to the equilibrium liquidus temperature. We also note that all points on the different curve whose abscissa is T_{end2} form a straight line $L_{T_{end2}}$ (see Fig. 6), which cuts the axis of abscissa at the equilibrium temperature $T_{eq}(X_{a,i}) = -2.8\,^{\circ}\mathrm{C}$ of the initial mixture for $X_{a,i} = 0.04$. The same result is obtained for T_{peak2}. We find that for different heating rates all points whose abscissa is T_{peak2} are aligned. The straight-line $L_{T_{peak2}}$ formed by these points cuts also the axis of abscissa at the equilibrium temperature $T_{eq}(X_{a,i}) = -2.8\,^{\circ}\mathrm{C}$ of the initial mixture. These results are evident because the more the heating rate decreases and becomes near to zero, the more the gradients of temperature within the sample become negligible.

In Fig. 7, T_{peak1} and T_{peak2} decrease continuously with decreasing heating rate and the distance D between $L_{T_{peak1}}$ and $L_{T_{peak2}}$ remains essentially constant. This effect on the peak temperatures is caused by the thermal resistance between the sample and the DSC platform. It may be noted that for every initial concentration of the NH_4Cl–H_2O system, the distance D is independent of the heating rate (see Fig. 7).

We note that when the initial fraction of the solute is close to the eutectic concentration $X_E = 0.195$, it is difficult to detect the end point of the progressive melting from experimental measurement. There are two main reasons for the difficulties. The

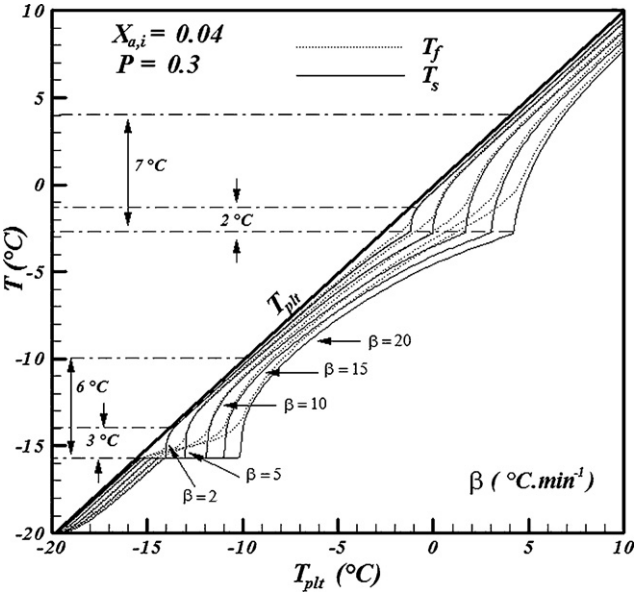

Fig. 3. Effect of the heating rate β on T_f and T_s in the center of the sample.

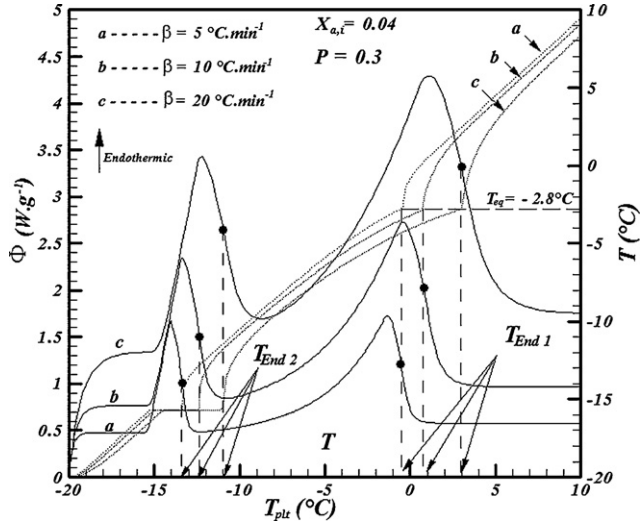

Fig. 5. Temperatures T_{end1} and T_{end2} for different β.

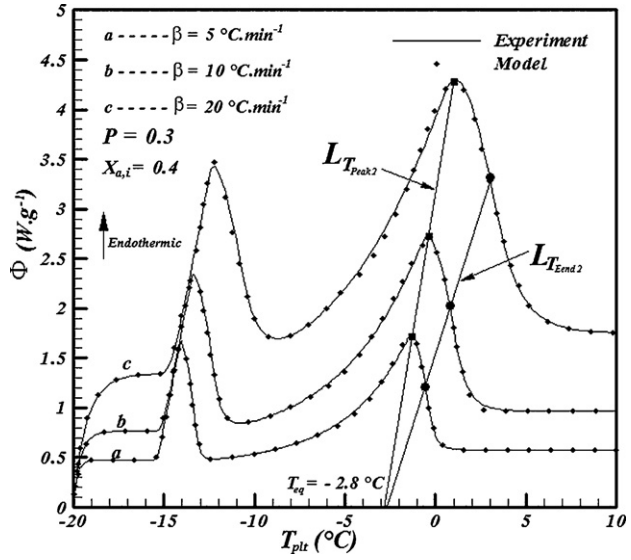

Fig. 6. Determination of the equilibrium temperature for $P = 0.3$, $X_{a,i} = 0.4$ and $\beta = 10\,^{\circ}\mathrm{C\,min^{-1}}$.

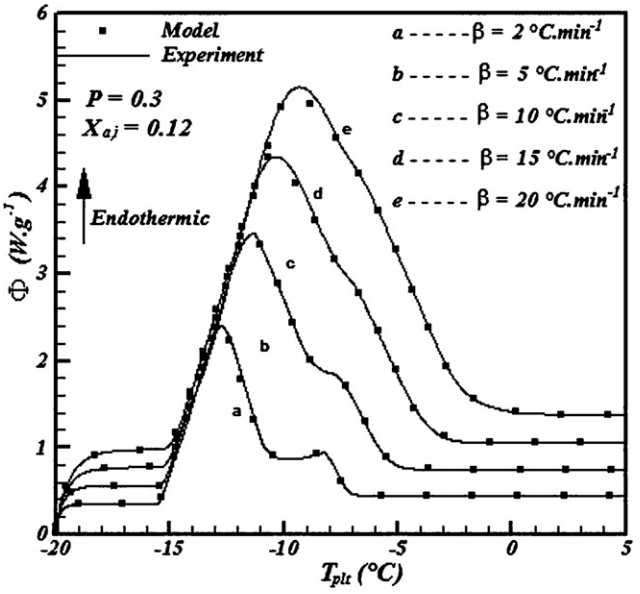

Fig. 8. Effect of the heating rate on the shape of the second peak for $P = 0.3$ and $X_{a,i} = 0.12$.

first one is due to the limited power of DSC to resolve two-phase transitions into distinct thermal peaks when the two transition temperatures are too close to each other. The second and the more serious is the grave imbalance between the quantities of the two phases whose temperatures are to be differentiated in a sample near the composition of convergence. In such a sample, thermal effect of phase transition for the phase of the larger quantity invariably overwhelms that of the smaller quantity [13]. In order to illustrate these difficulties, we have presented the numerical heat flow versus the heating rate for $X_{a,i} = 0.12$ (see Fig. 8). We note that the peak corresponding to the eutectic melting becomes larger when the heating rate increases. Increase in β leads to the disappearance of the second peak. It is clearly seen that the use of the high heating rate masque the information about the progressive melting. In order to describe with accuracy the end point of the progressive melting, it is desirable to use the lower heating rate.

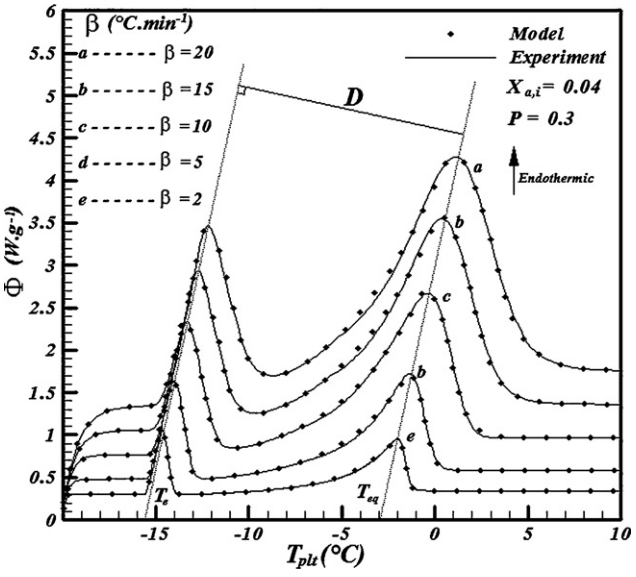

Fig. 7. Effect of the heating rate on the shape of the thermograms $P = 0.3$ and $X_{a,i} = 0.4$.

3.2. Effect of the initial mass fraction

For each initial mass fraction of the dispersed solution we have presented experimental and numerical heat flow (see Fig. 9). We note that the peak temperature of the progressive melting decreases with increasing initial mass fraction of the solute since the liquidus temperature decreases. When the initial mass fraction of the dispersed solution is much smaller than the eutectic concentration, the amount of the ice transformed during the eutectic melting is very little.

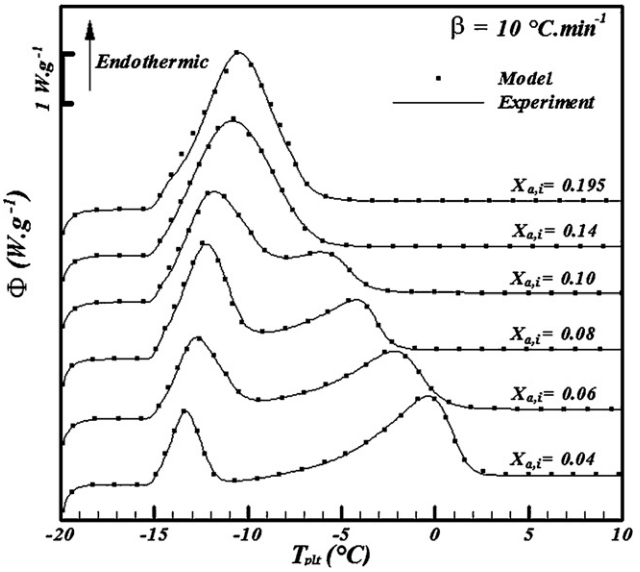

Fig. 9. Thermograms for different initial concentrations $X_{a,i}$.

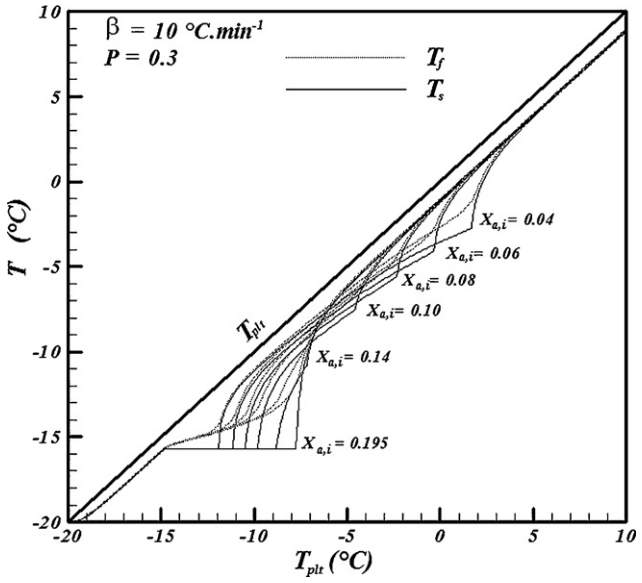

Fig. 10. Effect of $X_{a,i}$ on T_f and T_s in the centre of the sample ($\beta = 10\,^{\circ}\mathrm{C\,min^{-1}}$, $P = 0.3$).

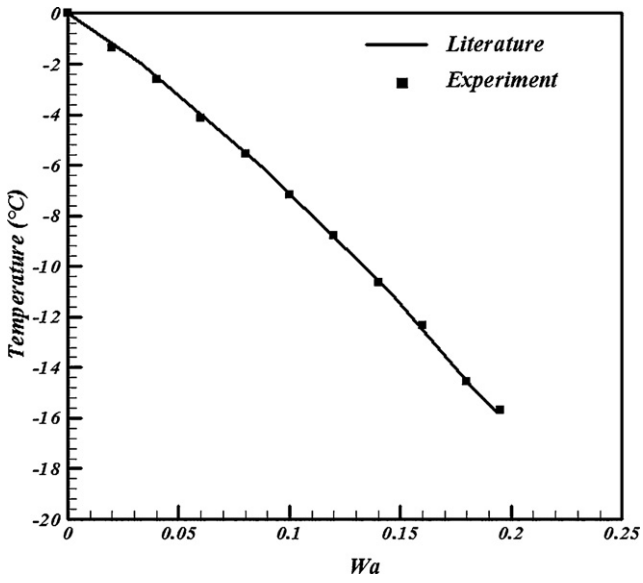

Fig. 12. Phase diagram of the NH_4–H_2O system: comparison between experiment results and literature data [10].

Fig. 10 displays the prediction of temperatures T_f and T_s in the center of the sample for different initial mass fractions. Despite the small dimensions of the sample, we have found important temperature gradients, responsible for the shape of the peaks. These gradients become more and more important as initial mass fraction increases.

Fig. 11 shows the distance D between $L_{T_{peak1}}$ and $L_{T_{peak2}}$ for different initial concentrations $X_{a,i}$. We note that D decreases continuously with increasing salt concentration.

For every initial concentration of the dispersed solution and for various heating rate, we have found that the equilibrium temperature of the initial mixture corresponds perfectly to the intersection of the two straight-lines $L_{T_{peak2}}$ and $L_{T_{end2}}$.

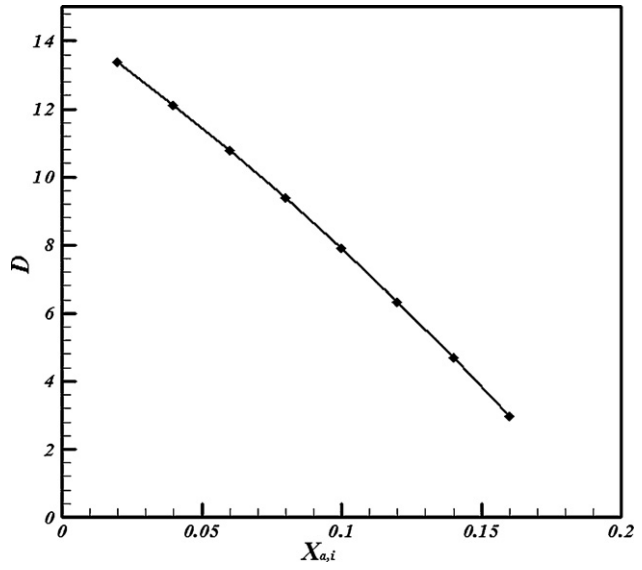

Fig. 11. Distance D between $L_{T_{peak1}}$ and $L_{T_{peak2}}$ for various initial concentrations $X_{a,i}$.

The results reveal that for the same initial concentration of the dispersed solution and using various heating rate we will be able to predict the solid–liquid equilibrium temperature of the initial mixture.

Fig. 12 illustrates the equilibrium liquidus temperatures of the NH_4Cl–H_2O system obtained from the DSC curves and the literature data [10]. The last one coincides perfectly with the experimental binary phase diagram.

4. Conclusion

The liquidus equilibrium temperatures were determined from thermal analysis using a differential scanning calorimeter and physical model. The transformed fraction of solution was evaluated by employing the proposed model. By employing the transformed fraction of the solution we can detect the end of both transformations: eutectic and progressing melting. Experiment results are in good agreement with the data provided by the literature. In order to describe with accuracy the heat transfer during the melting process inside an emulsion, it is desirable to use the lower heating rate.

References

[1] A. Jamil, T. Kousksou, Y. Zeraouli, J.P. Dumas, E. Schall, Isothermal and non-isothermal melting of the binary solution inside an emulsion, Thermochim. Acta 460 (2007) 22–27.
[2] M. Tang, W.H. Tao, C.C. Wu, Y.P. Chen, Solid–liquid equilibrium and heat capacity measurements of water + sodium bromide and water + sodium carbonate binary mixtures, J. Chin. Inst. Chem. Eng. 34 (2003) 599–603.
[3] M. Tang, W.H. Tao, C.C. Huang, Y.P. Chen, Measurements of the heat capacity and solid–liquid equilibrium of water–potassium chloride and water–magnesium chloride binary mixtures, J. Chin. Inst. Chem. Eng. 33 (2002) 469.
[4] H.W. Ryu, S.W. Woo, B.C. Shin, S.D. Kim, Prevention of supercooling and stabilization of inorganic salt hydrates as latent heat storage materials, Solar Energy Mater. Solar Cells 27 (1992) 161.

[5] H. Takiyama, H. Suzuki, H. Uchida, M. Matsuoka, Determination of solid–liquid phase equilibria by using measured DSC curves, Fluid Phase Equilib. 194 (2002) 1107–1117.
[6] A.R. McGhie, G.J. Sloan, J. Cryst. Growth 32 (1976) 60–67.
[7] M. Matsuoka, N. Kanekuni, H. Tanaka, J. Cryst. Growth 73 (1985) 563–570.
[8] C.C. Huang, Y.P. Chen, Measurements and model prediction of the solid–liquid equilibria of organic binary mixtures, Chem. Eng. Sci. 55 (2000) 3175–3185.
[9] O. Sassi, I. Siffrini, J.P. Dumas, D. Clausse, Theoretical curves in thermal analysis for the melting of binaries showing solid solution, Phase Trans. 13 (1988) 101–111.
[10] I. Siffrini, Phénomènes de cristallisation dans des solutions salines aqueuses à l'état dispersé et sous forme de gouttes, Thèse de Doctorat, Université de Pau et des Pays de.
[11] J.P. Dumas, Y. Zeraouli, M. Strub, Heat transfer inside emulsions. Determination of the DSC thermograms. Part 1. Crystallizations of the undercooled droplets, Thermochim. Acta 236 (1994) 227–237.
[12] J.P. Dumas, Zeraouli, M. Strub, Heat transfer inside emulsions. Determination of the DSC thermograms. Part 2. Melting of the crystallized droplets, Thermochim. Acta 236 (1994) 239–248.
[13] M.S. Ding, K. Xu, T.R. Jow, Phase diagram of EC DMC binary system and enthalpic determination of its eutectic composition, J. Therm. Anal. Calorimetry 62 (2000) 177–186.